ISSN 1063-7397, Russian Microelectronics, 2017, Vol. 46, No. 2, pp. 131–138. © Pleiades Publishing, Ltd., 2017.
Original Russian Text © A.S. Korotkov, V.V. Loboda, S.B. Makarov, A. Feldhoff, 2017, published in Mikroelektronika, 2017, Vol. 46, No. 2, pp. 142–150.

Modeling Thermoelectric Generators Using the ANSYS Software Platform: Methodology, Practical Applications, and Prospects

A. S. Korotkov[a], *, V. V. Loboda[a], S. B. Makarov[a], and A. Feldhoff[b]

[a] *Peter the Great St. Petersburg Polytechnical University, St. Petersburg, 195251 Russia*

[b] *Leibniz Universität Hannover, Germany*

**e-mail: korotkov@spbstu.ru*

Received March 17, 2016

Abstract—We present a review of modeling techniques of thermoelectric generators (TEGs) with the use of the finite element method based on the software of the ANSYS Workbench platform. Comparative analysis of different models and with the experiment is presented. The development direction of methods for studying the properties of promising TEGs, including generators based on MEMS technology, as well as segmented and coaxial types, is discussed. It has been shown that an important step in the design is to calculate the geometric parameters of the thermoelements (TEs) carried out with the help of numerical methods for solving the optimization problem by the criterion of maximizing the power output. The use of modeling techniques makes it possible to determine the activation modes of TEGs, operating temperature range, load resistance, and the output power.

DOI: 10.1134/S1063739717020056

1. INTRODUCTION

Thermoelectric generators (TEGs) are used as primary (autonomous) power sources in many practical applications with the required power ranging from mW units to W units. Fundamentals of TEG application were laid down already in classical works by A.F. Ioffe, Yu.P. Maslakovets and L.S. Stilbans [1]. Currently, TEGs are widely used in power supply systems for engine monitoring [2–4], biomedical equipment [5], etc. [6]. As a result, TEGs are fabricated by various manufacturers: Laird/Melcor (United Kingdom/United States), Ferrotec (Japan), Marlow (United States), Tellurex (United States); in the Russian Federation: Kryotherm, SKB Nord, PMT, Osterm, SPC Crystal, SPC RIF, and ADV-Engineering. The Fraunhofer Institute's annual report (ENAS) [7, p. 33] states: "... the simulation shows that TEGs can not only be designed with maximum efficiency but each TEG must be individually tuned for the respective purposes." In this regard, a necessary stage in the development of power sources is TEG modeling to determine the optimal parameters of its switching.

The purpose of this review is the comparative analysis of different approaches to the construction of models and determining practical recommendations in modeling TEGs, including advanced types—multilayered, coaxial, and those implemented based on the technology of microelectromechanical systems (MEMS). The paper is organized as follows. In the second section, after the introduction, general information and an overview of the peculiarities of TEGs are given. In the third section, we treat the aspects of TEG modeling based on the finite element method, performing a comparative analysis of different models and with the experiment. The fourth section presents the development trends and the methods for studying the properties of promising TEG types. In the conclusion, general conclusions and recommendations are given.

2. GENERAL INFORMATION ON TEGs

A TEG is a semiconductor device for directly converting heat into electricity. The principle of a TEG is based on the Seebeck effect [8, p. 14]. If the contact pads of semiconductor materials with a different type of conductivity (n- and p-type) are maintained at different temperatures and a TEG is connected to the external load, then the current flows through the circuit, and useful power is released in the load R_{H}. A TEG unit element is a pair of thermoelements (TEs) (Fig. 1). It consists of TE pairs connected in series, arranged between two ceramic plates. The TEs are connected by metallic contact pads (Fig. 2).

Thermoemf voltage E_{Temf} is directly proportional to the Seebeck coefficient of generator α and temperature difference ΔT between the hot T_h and cold T_c sides of a TEG:

$$E_{\text{Temf}} = \alpha \Delta T.$$

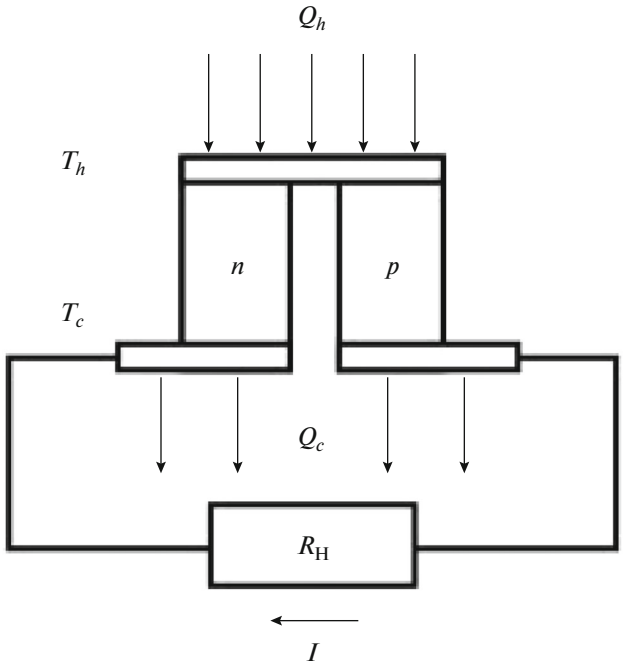

Fig. 1. Scheme of a TEG based on one pair of TEs.

The voltage U created on the external load R_H equals emf with the subtraction of the fall in voltage on the inner resistance R of the generator:

$$U = E_\text{Temf} - IR,$$

where the current I in the circuit is given by

$$I = \frac{\alpha\Delta T}{R + R_\text{H}} = \frac{\alpha\Delta T}{R(1+m)},$$

and parameter $m = \frac{R_\text{H}}{R}$ is:

$$U = IR_H = \alpha\Delta T\frac{m}{1+m}.$$

The power released in the external circuit is calculated by the formula

$$P = UI = \frac{\alpha^2\Delta T^2}{R}\frac{m}{(1+m)^2}.$$

To create the difference of the temperature on the sides of a TEG, the heat flux Q_h should arrive on the hot side, while the heat flux Q_c should leak out of the cold side. The difference between these heat fluxes according to the energy conservation law is equal to the electric power P:

$$P = Q_h - Q_c.$$

The efficiency of a TEG is given by

$$\eta = \frac{P}{Q_h}.$$

The heat flux Q_h can be found from the heat balance equation. In addition to the heat flux Q_h, half of the Joyle heat scattered in the branch of TE also arrives on the hot side. However, due to the Peltier effect, at the point of contact between the semiconductor and the metal, the amount of heat equal to αIT_h is absorbed. Furthermore, the heat conduction mechanism in the branches takes place from the hot side to the cold one which leads to the additional release of heat proportional to the heat conductivity K_m of the generator (see below). Therefore, the heat balance equation of the hot side takes the form

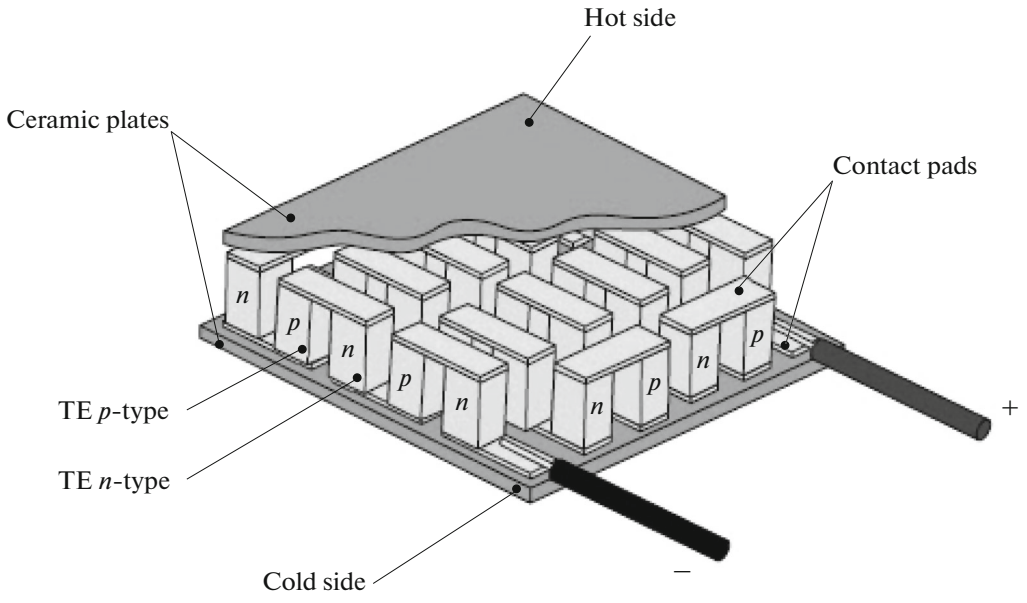

Fig. 2. Structure of a TEG.

$$Q_h + \frac{1}{2} I^2 R = \alpha I T_h + K_m \Delta T, \quad (1)$$

whence it follows

$$Q_h = K_m \Delta T \left(1 + \frac{Z T_h}{1+m} - \frac{1}{2} \frac{Z \Delta T}{(1+m)^2} \right),$$

where $Z = \frac{\alpha}{R + K_m}$ describes the performance of the semiconductor material. Analogously to that, the heat flux Q_c is given by

$$Q_c = K_m \Delta T \left(1 + \frac{Z T_c}{1+m} + \frac{1}{2} \frac{Z \Delta T}{(1+m)^2} \right).$$

The efficiency η has the form

$$\eta = \frac{T_h - T_c}{T_h} \frac{1}{1 + \frac{1}{m} + \frac{1}{Z T_h} \frac{(1+m)^2}{m} - \frac{1}{2} \frac{T_h - T_c}{T_h} \frac{1}{m}}. \quad (2)$$

Equation (2) means that the efficiency of a TEG is determined by the efficiency of the Carnot cycle and the factor depending on m, Z, and temperatures T_h and T_c. This factor is less than 1, and for the present day quality of semiconductor materials, it is about 0.15. The choice of parameter m determines the efficiency and the output electric power of a TEG. The maximum power is reached at equal values of external and internal load ($m = 1$). The maximum efficiency corresponds to the following value of m:

$$m = \sqrt{1 + Z \frac{T_c + T_h}{2}} \approx 1.3\text{–}1.4.$$

A TEG is characterized by the following parameters:

$$R = N (\rho_n + \rho_p) \frac{h}{a^2} = N (\rho_n + \rho_p) \gamma, \quad (3)$$

where N is the number of TE pairs, h is the height of a TE, a is the side of a TE cross section, $\gamma = \frac{h}{a^2}$ is the geometrical factor, ρ_n and ρ_p is the specific electric resistance corresponding to n- and p-type TEs, correspondingly; thermal conductance

$$K_m = N \frac{(\lambda_n + \lambda_p)}{\gamma}, \quad (4)$$

where λ_n and λ_p are the thermal conductivities of n- and p-type TEs, respectively; Seebeck coefficient

$$\alpha = N \left(\alpha_T^p - \alpha_T^n \right), \quad (5)$$

where α_T^n and α_T^p are the Seebeck coefficients of the n- and p-type TEs, correspondingly.

Semiconductor TE materials providing the highest conversion ratio of heat into electricity are used in TEG fabrication. The maximum efficiency of thermoelectric material is determined by a dimensionless parameter: the product of thermoelectric efficiency Z and temperature T. The maximum values of ZT for semiconductor materials lie in the range of 0.8–1.1, and the higher values are reached for p-type semiconductors (Fig. 3).

3. CONSTRUCTING A THERMOELECTRIC GENERATOR MODEL USING ANSYS

Solving the problem of modeling is based on the finite element method with the use of the ANSYS Workbench platform. The process of modeling involves the following stages: preprocessing, solving, and postprocessing the results. The stage of preprocessing involves five steps: construction of a geometric 3D-model of the object using the ANSYS Design Modeler designed for constructing, editing geometry, and assigning the attributes of models; the choice of the type of analysis—thermal-electric analysis as applied to TEG modeling; setting the physical properties of materials that make up a simulated object (engineering data); creating the model of a solid state object using the ANSYS Mechanical module, which allows us to determine the temperature field by solving the problems of stationary and nonstationary heat conduction, convection, and radiation heat transfer; and generation of a finite element mesh using the module ANSYS Meshing. The stage of obtaining the solution consists of the following steps: the choice of the type of analysis (Steady-State Analysis) and options for the type of analysis chosen at the preceding stage; the choice of the boundary conditions: thermal and electrical; and the choice of the calculation parameters. At the final stage, the results are displayed in graphical and tabular form.

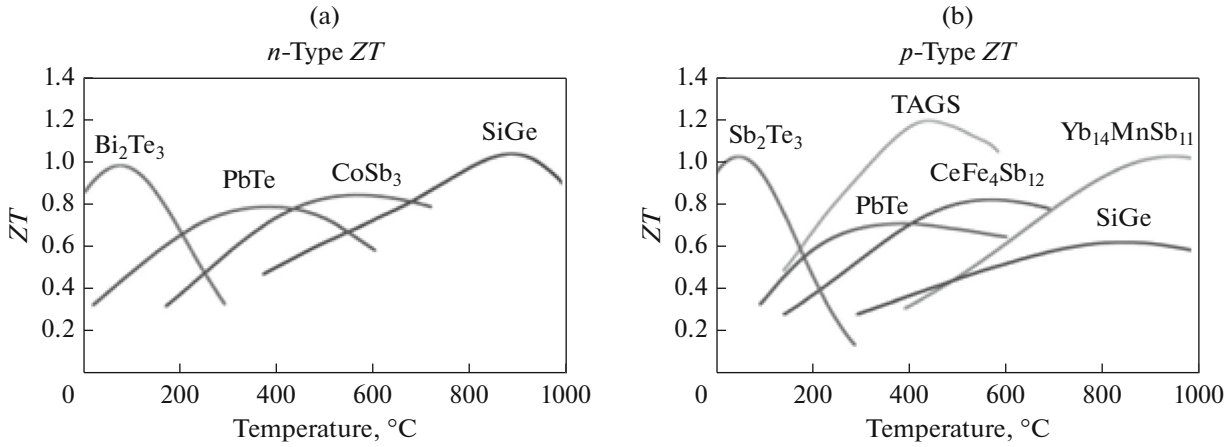

Fig. 3. Thermoelectric index ZT for commercial materials [9]: (a) n-type; (b) p-type.

This methodology is used in the simulation of TEGs in [10–19]. As an object of modeling in [10], a TEG with two TEs was considered with the following set of parameters and geometry: ρ_n, ρ_p, λ_n, λ_p, α_T^n, and α_T^p (see expressions (3)–(5)). Modeling was carried out at the following boundary conditions: $T_c = 27$°C and $T_h = 327$°C. Two models were built differing in the way the physical parameters of the materials were set. In model 1, the temperature was assumed to be constant and equal to the average median temperature of the TE. In model 2, the temperature dependence of the parameters was introduced with allowance for the boundary conditions. It should be noted that the simulation was carried out without consideration of the contact resistance between the branches of the TE and contact metal pads. The simulation results were compared with the theoretical calculation. It is shown that the introduction of the temperature dependence of the parameters provides a correction of up to 15%.

In [11], two commercial TEGs (Thermomatic Co.) were modelled. The first TEG, namely, TEHP1-12680-0.15, has linear dimensions of 80 × 80 mm and contains 126 TE pairs. The second TEG has dimensions of 40 × 40 mm and contains 127 TE pairs. The physical parameters of the TEG materials given in the technical description of the generator's manufacturer were put into the model. The temperatures T_h and T_c on the surface of the ceramic wafers were set as the thermal boundary conditions. The simulation was performed with the load resistance equal to the internal resistance of the generator, which corresponds to the maximum of the output power. The authors presented two models: model 1 without accounting for the metal-semiconductor electric contact resistance and the thermal resistance of the metal-ceramic contact; model 2 was given with allowance for all contact resistances. The values of the contact resistances were calculated using regression analysis. The modeled parameters were voltage; current; heat flux flowing through a TEG; and power. The calculation results for models 1 and 2 shows a discrepancy in the output values ranging from 50 to 200%, depending on the temperature difference on the hot and cold sides. In addition, the experimental validation of the TEG parameters demonstrates the compliance of model 2 (with allowance for all resistances) and the experimental results with an accuracy of up to 2–3%. Thus, accounting for the contact resistance in the construction of the TEG model is necessary.

In [12], a GM200-71-14-16 TEG (European Thermodynamics), having 71 TE pairs and linear dimensions of 30 × 30 mm, was selected for the computer and experimental analysis. The authors presented three models for analyzing the characteristics of a TEG and conducted comparative analysis of the simulation results, and the experimental and manufacturer data. The geometric 3D model is a TEG for models 1 and 2 and a TEG with a heat spreader on the hot side, the role of which is played by an aluminum wafer for model 3. The thermal boundary conditions and the corresponding planes were selected as follows. In model 1, temperatures T_h and T_c were set on the surfaces of the ceramic plates. In model 2, the heat flux Q_h was set on the surface of the hot ceramic plate and temperature T_c was set on the surface of the cold ceramic plate. In model 3, the heat flux Q_h was set on the surface of the aluminum heat spreader on the hot side of the TEG, and temperature T_c was set on the surface of the cold ceramic wafer. Temperature T_c in all three cases was 30°C. The heat flux Q_h was calculated using the heat balance equation on the hot side according to (1), and using the value of the current obtained in model 1. In all three models, natural convection was introduced except for the TEs. The physical parameters of the TEG material used in all the models are given in the manufacturer's technical description of the generator. The calculation was performed when the output power of the TEG reached

the maximum, and the load resistance was equal to the internal resistance of the generator. At the first stage of modeling, the calculations were carried out under the following thermal boundary conditions: $T_h = 200$°C in model 1, $Q_h = 56.4$ W in models 2 and 3 (the heat flux was calculated by formula (1) at a current value of 1.42 A, calculated using model 1). The calculation results showed the following deviations from the manufacturer's data in the power value: 36.5% (model 1), 5.9% (model 2), and 7.1% (model 3). At the second stage of modeling, the distribution of the temperature on the surfaces of the ceramic plate (model 2) and heat flux spreader (model 3) into which the heat flux enters was taken into account. The presence of the temperature gradient was found in model 2 on the surface of the ceramic plate: the temperature varies from 199°C at the center to 169.5°C at the edges. In model 3, the gradient of the temperature distribution on the surface is lower, and the maximum temperature is also lower: 179°C and 174°C at the center and at the edges of the aluminum plate, respectively. Thus, to compare the calculation results for all three models, the boundary condition for T_h was corrected in model 1 and the calculation was performed at a temperature of 176°C of the hot TEG side, which corresponds to the average temperature of the surface in models 2 and 3. As a result, the power deviation in model 1 from the manufacturer's data was 7.4%. This approach was used further in calculating the parameters of the generator, using all three models at different temperatures on the hot side of the TEG. Comparing the simulation results with the experimental data and those of the manufacturer for the output power shows that all three models coincide within the range of 2–3 and 5–7%, respectively. From these results one can conclude that all three models allow us to adequately and accurately describe the TEG operation.

In [13], the authors modeled the TEG parameters with allowance for the design components of the experimental setup: the heater of the cold side was a copper plate with three holes for water circulation (cold unit); and the heater of the hot side was a copper plate with an electric heating element for the TEG inside (hot unit). For modeling, a geometric model, including a TEG with 127 TE pairs, the cold and hot units, and the load, was built. The boundary conditions for the cold unit were set by the temperature of the circulating water in the holes (19°C), a convection coefficient of 1376.4 W/m^2 K calculated based on the adjoint thermal analysis using the ANSYS CFX software, the value of the current fed on the electric element of the heater in the hot unit, and the natural convection of all parts of the construction without the cold unit. The physical parameters of the materials were taken from the literature. The model also takes into account all the electric and thermal resistances. A feature of the results is the modeling of the transition process from the initial state without switching the heater to the steady state at a fixed temperature. It is shown that under the given conditions the duration of transition process is about 4000 s. The output power was about 4 W when the temperature difference across the plates was 150°C.

As a result of simulation, the temperature distribution in the volume and along the surface of the cold and hot blocks, as well as the profiles of the output voltage, current density, Joule heating, and temperature for the TEG, were determined.

Work [14] is devoted to the simulation and experimental analysis of the TEC 1-7105 TEG (Conrad Electronics SE) having 71 TE pairs and linear dimensions of 30 × 30 mm. The model was built using the ANSYS Parametric Design Language. The model represents a single TEG. The boundary thermal conditions are set by the temperatures T_h and T_c on the surfaces of the ceramic wafers. The physical parameters of the semiconductor materials, namely, ρ_n, ρ_p, λ_n, λ_p, α_T^n, and α_T^p were determined by solving the problem of parameter extraction according to the results of the experiment. The material parameters of the contact pads and ceramic wafers were taken from the ANSYS library. In contrast to the aforementioned works, the simulation and experiment were carried out in the range of loads from 1 Ohm to 10 kOhm in five temperature regimes and a temperature difference across the plates of 58, 43, 33, 25, and 13°C (Fig. 4).

It is shown that under the condition of the maximum power transfer to the load, the TEG output power is 145, 90, 47, 23, and 4 mW, respectively (the data were obtained by averaging the results of three measurements). The difference between the results of the modeling and experimental data does not exceed 3%. The presented approach allows one to extrapolate the reference data for a commercially available TEG and, therefore, to select a generator with allowance for the given conditions for the power and operating temperatures. It is to be noted that the software with the same functional purpose allowing simulation of the output TEG characteristics is protected by the certificate of state registration [15].

4. MODELING TYPES OF TEGs WITH PROMISING PROSPECTS

4.1. Trends in the Development of TEGs

The main trends in the development of TEGs are microminiaturization of the TEG design and increasing efficiency. These problems are solved by using the new technological principles of TEG construction and improving the TE design and geometry. In the first case, the use of MEMS technology is critical, and in the second case, the use of numerical methods for solving the optimization problem in the construction of the TEs. The ANSYS Workbench platform includes a specialized optimization ANSYS DesignXplorer

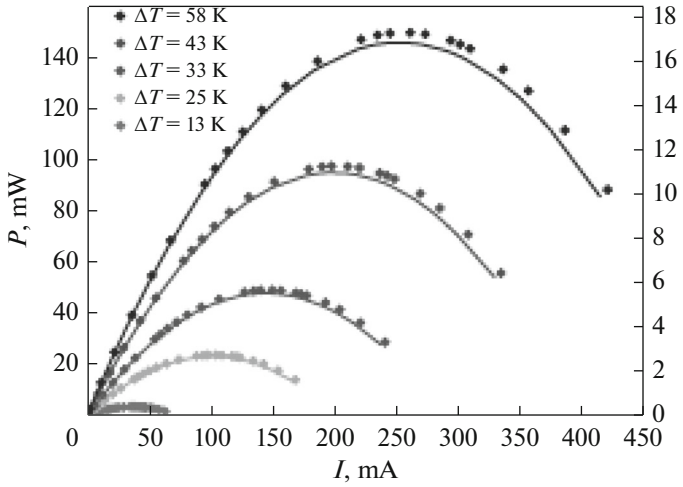

Fig. 4. Dependences of the output power on the load current in various temperature regimes (the points correspond to the experiment; and the lines correspond to the modeling) [14].

module. Two optimization techniques are used: direct and across the response surface. The solution is carried out using the following optimization algorithms: MOGA (multicriteria genetic algorithm), NLPQL (nonlinear programming with quadratic Lagrange functions), MISQP (mixed integer sequential quadratic programming), and others.

Note that a particular problem is the choice of TE materials, as discussed in detail, for example, in [16]. When constructing a TE, they are separated onto several parts, which generally can be made of different materials. A TEG is segmented or multilayered [17, 18] in the case of the arrangement of its elements by height. A TEG is coaxial if the thermoelectric construction is a nested system of several TEs [19]. Next, consider the details of the TEG modeling of segmented and coaxial types based on MEMS.

4.2. Features of Modeling MEMS-Based TEGs

The authors of [20, 21] applied the simulation methodology to the TEG described above, implemented based on the MEMS technology. As an object of modeling, a HV56 TEG (Nextrem Thermal Solutions Co.) with 72 TE pairs of TEs was used. The geometrical dimensions of the TEG parts and the physical parameters of the materials were taken from the datasheet of the TEG manufacturer. The temperatures T_h and T_c on the surfaces of the ceramic plates were used for the boundary conditions. The temperature field distribution and the output voltage of the TEG were calculated at a load resistance equal to the internal resistance of the generator corresponding to the maximum output power. Comparing the modeling results of the output voltage with those for the generator model obtained using MATLAB/Simulink and with the manufacturer's data shows a coincidence within the limits of 8 and 12%, respectively.

It should be noted that the published results allows one to perform a comparative analysis of the main TEG parameters based on the discrete components and MEMS technology. Based on this, we can make the following conclusions which confirm the results of the modeling and experiment:

(1) The operating temperature range for TEG based on the discrete components typically ranges from 0 to 250°C, which is about twice as high as the operating temperature range for a TEG based on MEMS technology. Moreover, the critical temperatures range from 350 to 260°C.

(2) When the output power is maximized, the absolute output power released on the load in the case of a TEG based on the discrete elements exceeds as a rule, the power for a MEMS-based TEG. However, by the parameter of specific power, i.e., the total power with respect to the working surface area, a MEMS-based TEG greatly exceeds a TEG based on discrete components, by a factors ranging between four and five, for example.

4.3. Features of Modeling Segmented TE Generators

When constructing segmented TEGs, the optimization problem is solved by maximizing the output power of TEGs at the given temperature difference ΔT. As the optimization parameters, the geometrical sizes of the parts of a TE are considered. In [17], the TEG model has measures 40 × 40 mm and consists of 254 TEs. Each TE is separated into two parts. The parts of the *n*-type and *p*-type TE are designated as "*n*-type-cold," "*n*-type-hot," "*p*-type-cold," and "*p*-type-hot," depending on the location relative to the cold and hot ceramic plates. Each part is described by a geometrical parameter:

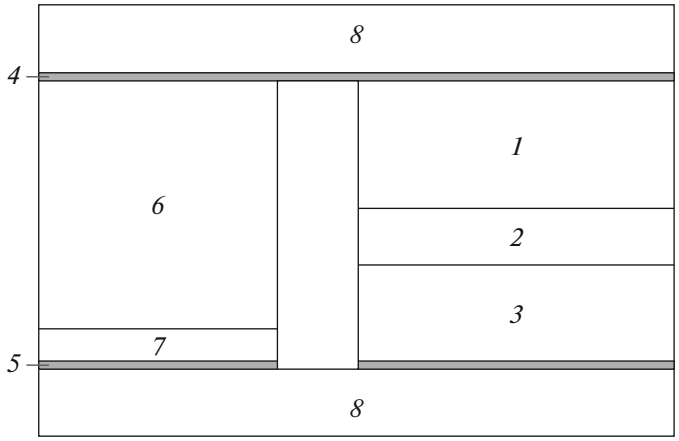

Fig. 5. Structure of a segmented TEG: *1*—*p*-$CeFe_4Sb_{12}$; *2*—*p*-Zn_4Sb_3; *3*—*p*-Bi_2Te_3; *4*, *5*—Cu; *6*—*n*-$CoSb_3$; *7*—*n*-Bi_2Te_3; *8*—Al_2O_3 [18].

variable height with fixed crosssection and total height. Each part has its own prescribed parameter *ZT*. The cross-sectional area of a TE is 1.4 × 1.4 mm and the total height is 1.5 mm, including the copper contact between the TE parts. A variable parameter in the process of optimization is the height of the *n*-type-cold and *p*-type-cold parts. The height was varied in the range from 0.1 to 1.4 mm with a step of 0.1 mm. The temperatures T_h = 170°C and T_c = 20°C on the surface of the ceramic plates were set as the boundary thermal conditions. As a result of the solution, the optimal value of 0.7 mm was obtained for the height of the *n*-type-cold and *p*-type-cold parts. Moreover, the output power was 6.15 W, that is, 8% higher than the power for a nonsegmented TEG with the same linear dimensions.

In [18], a more complicated TE structure is considered for high-temperature applications (up to 780 K) consisting of four TE pairs. The geometrical dimensions of the TEs were determined using the criterion of the maximum output TEG current. In particular, a *p*-type TE with a cross section of 8 × 8 mm was separated into three parts: with a thickness of 3.7 mm (based on $CeFe_2Sb_{12}$), 1.6 mm (based on Zn_4Sb_3), and 2.8 mm (based on Bi_2Te_3). An *n*-type TE with a cross section of 6 × 6 mm was separated into two parts with a thickness of 7.2 mm ($CoSb_3$-based) and 0.9 mm (Bi_2Te_3-based) (Fig. 5). As the thermal boundary conditions, the temperature T_c = 300 K on the surface of a cold ceramic plate and a heat flux of 15 W were chosen. The output voltage is 0.845 V at a load resistance of 0.06 Ohm. Segmentation of the TEG TEs enabled us to increase the efficiency up to 10%.

4.4. Features of Modeling Coaxial TEGs

In [19], the comparative analysis and modeling of two types of TEs are carried out, each of them consisting of a cylindrical TE. A TEG of type 1 involves four cylindrical TEs with a thickness of 3.0 mm and a diameter of 1.6 mm. A TEG of type 2 is represented by two structures having four coaxial TEs with a height of 3 mm. The internal TEs are fabricated as cylinders with a diameter of 1.6 mm, and the external TEs are formed as cylindrical tubes with different internal and external diameters of 2.0, 2.4 mm, and 2.56, 2.88 mm, respectively. Therefore, all the modeled TEGs have the same cross-sectional area of 2 mm^2. The temperatures T_h = 120°C and T_c = 20°C, and an external convection of 10 W/m^2 were set as the thermal boundary conditions on the surface of the ceramic plates. The material's parameters were taken from the literature. The following parameters were simulated: temperature distribution, the density of the current flowing through the TE, and the heat flux on the hot surface of the ceramic plates. The output power and efficiency were calculated according to the simulation results. It was shown that the output power and efficiency of the thermogenerators of the first and second type are close to each other. The difference in the output power and efficiency proved to be of the order 2% and a fraction of a percent, respectively.

CONCLUSIONS

The analysis shows that two programs are mainly used for the simulation of TEGs to which the finite element method is applied, namely, the ANSYS Workbench platform and COMSOL Multiphysics. The ANSYS Workbench platform makes it possible to use the embedded moduli in solving various physical problems. It is used more frequently in practice. The use of modeling techniques allows one to determine the most effective parameters of switching TEGs, such as the operating temperature range, load resistance, and power output. An important step in the design of TEGs is the calculation of the geometric parameters of the TEs, carried out with the help of numerical meth-

ods when solving the optimization problem by the criterion of maximizing the power output of TEGs.

REFERENCES

1. Fedorov, M.I., Vedernikov, M.V., and Iordanishvili, E.K., A.F. Ioffe and thermoelectricity in Physical Technical Instituite, in *Peterburgskaya-leningradskaya shkola elektroniki* (Petersburg-Lenigrad School of Electronics), Collection of Articles, Alferov, Zh.I., Ed., St. Petersburg: SPbGETU "LETI", 2013, pp. 216–226.
2. Vinogradov, S.V., Khalykov, K.R., and Kong Doan Nguen, Method of calculation and estimation of parameters of the experimental thermoelectric generator, *Vestn. Astrakh. Tekh. Univ., Ser.: Morsk. Tekh. Tekhnol.,* 2011, no. 1, pp. 84–91.
3. Sysoeva, S.A., Devices for wireless and batteryless power of autonomous units. Part 2, *Elektron. Komp.,* 2011, no. 7, pp. 81–84.
4. Janak, L., Ancik, Z., Vetiska, J., and Hadas, Z., Thermoelectric generator based on mems module as an electric power backup in aerospace applications, *Mater. Today: Proc.,* 2015, vol. 2, pp. 865–870.
5. Ben Hmida, G., Ekuakille, A.L., Kachouri, A., Ghariani, H., and Trotta, A., Extracting electric power from human body for supplying neural recording system, *Int. J. Smart Sens. Intell. Syst.,* 2009, vol. 2, no. 2, pp. 229–245.
6. Vullers, R.J.M., van Achaijk, R., Visser, H.J., Penders, J., and van Hoof, C., Energy harvesting for autonomous wireless sensor networks, *IEEE J. Solid-State Circuits,* 2010, pp. 29–38.
7. *ENAS Annual report 2013,* Gessner, Th. and Vogel, M., Eds., Chemnitz: Fraunhofer Inst. Electronic Nano Systems (ENAS), 2013, p. 107.
8. Ioffe, A.F., *Poluprovodnikovye termoelementy* (Semiconductor Thermal Cells), Moscow: Akad. Nauk SSSR, 1960.
9. Snyder, G.J. and Toberer, E.S., Complex thermoelectric materials, *Nat. Mater.,* 2008, vol. 7, pp. 105–114.
10. Antonova, E.E. and Looman, D.C., Finite element for thermoelectric devices in ANSYS, in *Proceedings of the 24th International Conference on Thermoelectronics ICT'05, Clemson, USA,* 2005, pp. 215–218.
11. Hogblom, O. and Andersson, R., Analysis of thermoelectric generator performance by use of simulations and experiments, *J. Electron. Mater.,* 2014, vol. 43, no. 6, pp. 2247–2254.
12. Kossyvakis, D.N., Vossou, C.G., Provatidis, C.G., and Hristoforou, E.V., Computational and experimental analysis of a commercially available seebeck module, *Renewable Energy,* 2015, vol. 74, pp. 1–10.
13. Li, W.-G., Paul, M.C., et al., Multiphysics simulations of a thermoelectric generator, *Energy Proc.,* 2015, vol. 75, pp. 633–638.
14. Geppert, B., Groeneveld, D., Korotkov, A., Loboda, V., and Feldhoff, A., Finite-element simulations of a thermoelectric generator and their experimental validation, *Energy Harvesting Syst.,* 2015, vol. 2, no. 1, pp. 94–105.
15. Loboda, V.V. and Korotkov, A.S., The program for simulation of modules of multielement thermoelectrical generators, State Registration Certificate on Computer Software, 2015, no. 2015661985.
16. Dmitriev, A.V. and Zvyagin, I.P., Current trends in the physics of thermoelectric materials, *Phys. Usp.,* 2010, vol. 53, no. 8, pp. 789–803.
17. Picard, M., Turenne, S., Vasilevskiy, D., and Masut, R.A., Numerical simulation of performance and thermomechanical behavior of thermoelectric modules with segmented bismuth-telluride-based legs, *J. Electron. Mater.,* 2013, vol. 42, no. 7, pp. 2343–2349.
18. Ming, T., Wu, Y., Peng, C., and Tao, Y., Thermal analysis on a segmented thermoelectric generator, *Energy,* 2015, vol. 80, pp. 388–399.
19. Erturun, U. and Mossi, K., Thermoelectric devices with rotated and coaxial leg configurations: numerical analysis of performance, *Appl. Therm. Eng.,* 2015, vol. 85, pp. 304–312.
20. Ancik, Z., Vlach, R., Janak, L., Kopecek, P., and Hadas, Z., Modeling, simulation and experimental testing of the MEMS thermoelectric generators in wide range of operational conditions, *Proc. SPIE,* 2013, vol. 8763, p. 87631M1.
21. Janak, L., Ancik, Z., and Hadas, Z., Simulation modelling of MEMS thermoelectric generators for mechatronic applications, *Mechatronics,* 2013, pp. 265–271.

Translated by G. Dedkov